

# IDENTIFICATION OF CONSTITUTIVE PROPERTIES OF COMPOSITE MATERIALS UNDER HIGH STRAIN RATE LOADING USING OPTICAL STRAIN MEASUREMENT TECHNIQUES

M. L. Longana\*<sup>1</sup>, J. M Dullieu-Barton<sup>1</sup> and F. Pierron<sup>1</sup>

<sup>1</sup> School of Engineering Sciences, University of Southampton, Southampton, Hampshire SO17 1BJ, UK  
\* mll1c09@soton.ac.uk

**Keywords:** High strain rate testing, Material characterisation, Full-field optical techniques, Virtual fields method.

## Abstract

*The paper describes experimental work that establishes a methodology for characterising the mechanical behaviour of glass fibre reinforced plastics at high strain rates. The experimental work is carried out using a high speed servo-hydraulic tensile test machine. Two optical strain measurement techniques, Digital Image Correlation (DIC) and the Grid Method (GM), are used to identify the strain field. The experimental work is described in detail and provides a practical description of how to obtain and process the optical data. The conclusion is a set of validated results that characterise the Young's Modulus of a GFRP at different strain rates.*

## 1 Introduction

The use of fibre-reinforced plastics (FRP) is increasing in a wide variety of structural applications, for instance, aerospace, marine, automotive and civil. Another field where the application of composite materials is attracting considerable interest is in blast or explosion protection and mitigation. Even if not specifically designed for this purpose, during their lifetime, all the structures in the traditional engineering fields mentioned above are subjected to high impulsive loads, such as manoeuvring loads, wave impacts, collisions or earthquakes. During these events, the material is often subjected to high loads at high strain rates. Even though it is well established that FRP behaviour is highly dependent on strain rate [1, 2], and various aspects of the high strain rate behaviour of composite materials have been studied [3, 4], most structural designs are based on material properties obtained from quasi-static tests run at low strain rates.

A complete review on techniques to test composite materials at high strain rates was compiled by Hamouda and Hashmi [5], while the techniques used to assess the tensile properties of composite materials at different strain rates have been summarised by Sierakowski [6]. The most widely used technique to test the high rate response of composite materials is the Split Hopkinson Pressure Bar (SHPB), because of its simplicity of usage. This approach allows very high strain rates to be achieved but critical issues arise with respect to mounting the specimen onto the machine and the size of the material to be tested is limited to a relatively small coupon. Bardenheider and Rogers [7] stated that servo-hydraulic machines give access to an intermediate strain rate range, difficult to apply with the other testing techniques. Nowadays, servo-hydraulic high rate test machines allow actuator speeds from quasi-static to 25 m/s to be achieved. This means the typical test duration may range from 10 to 10<sup>-5</sup> s and

strain rates between  $10^{-3}$  and  $10^3$  can be applied. The behaviour of composite materials within the strain rate range achievable with servo-hydraulic machines has not been investigated in great depth, apart from the work of Wang et al. [8], Fitoussi et al. [9], and Shokrieh and Omid [10].

Optical techniques are being increasingly used for displacement and strain measurements. These measurement methodologies evaluate deformation and strains by comparing the digital images of deformed and undeformed surfaces. Often a pattern, either regular or stochastic depending on the used technique, is applied to the surface to allow image comparison [11]. Over the last decade, the development of high speed cameras has made it possible to capture images with high temporal resolution leading to the use of optical techniques for the characterisation of materials at high strain rates. The advantages of such techniques are the absence of mechanical interaction between the measurand and the sensor, the possibility to obtain the full strain-displacement field and to experimentally determinate all the components of strain (normal and shear) on the observed surface. Grediac [11, 12] describes the importance of application of full-field methods in the modelling of composite material behaviour. Full-field techniques enable the relaxation of the restrictions on specimen dimensions and loading conditions. Moreover, knowing the complete stress-strain field allows the identification of heterogeneities in the field and allows their inclusion in a model. Furthermore, full-field techniques have the potential to reduce the number of experiments and sensors required to identify all the parameters for characterising an anisotropic material [11]. The aim of the work described here is to devise an experimental methodology to test FRP at strain rates of up to  $200 \text{ s}^{-1}$ . The material behaviour is characterised by deriving the Young's modulus at different strain rates from the material stress-strain data obtained during imaging.

## 2 Testing methodology and materials

### 2.1 Optical techniques

Two different techniques are used for obtaining the full-field strain map of the specimen surface are used in this work: the Digital Image Correlation (DIC) [13] and the Grid Method (GM) [14, 15]. The two techniques are different, but both rely on kinematic measurements, i.e. they provide displacement vectors, so it is possible to compare them in terms of spatial resolution, strain resolution and ease of use. DIC works by tracking the movement of grey levels in a sequence of images. To evaluate the displacements, the reference image of undeformed specimen surface, which is prepared by applying a painted speckle pattern to enhance contrast, is divided into interrogation cells, or subsets. The strain resolution is dependent on the size of the subsets and on their eventual superposition. The GM is based on fringe analysis, which is carried out three steps: the identification of the phase, the displacement evaluation, and the strain derivation. The fringes are directly applied on the specimen in the form of a regular grid transferred on the specimen. The phase is identified by analysing the light intensity at each pixel of the imaging sensor. The in-plane displacement is directly related to the carrier phase modulation and the strains are obtained spatially deriving the displacement.

It is important to remark that both DIC and GM are affected by common features that may result in distorted images being acquired that will result in incorrect strain derivations:

- Background noise: heat from the illuminating system, vibrations from the machine or the environment, voltage fluctuation in the imaging sensor and other random phenomena causes each sensor in the detector array to have biased image acquisition. As it is not

possible to mitigate the effect of the background noise it is important to understand its impact on the evaluated strain.

- Out of plane movement: two-dimensional strain measurement optical techniques that utilize only a single camera are not able to detect a movement of the specimen in the third direction and account for it during the processing. During the test, the specimen may be subjected to movements and rotations that vary the distance between the lens and the specimen, resulting in a change of magnification interpreted as a strain when analysing the images. Pannier et al. [16] established a linear relationship between out-of-plane movement and the parasitic strain induced by the out-of-plane movement as

$$\varepsilon_{\text{parasitic}} = dz/z$$

where  $z$  is the distance between the specimen and the lens and  $dz$  is the out of plane movement. This source of error in the measurement method is the believed to be the most severe.

### 2.2 High speed imaging

To perform material characterisation experiments at high strain rate using optical techniques it is necessary to acquire images at high frame rate. Various electronic devices, such as complementary metal-oxide semiconductors (CMOS) or charge coupled device (CCD) are used to capture digital images. The common feature in all these devices is that they are subject to noise coming from the electronic circuits used to intensify and capture the light and to convert it to a digital signal.

When imaging at high speed it is important to achieve a suitable compromise between the camera resolution and the frame rate to optimize the camera memory usage. A correct shutter speed must be chosen to acquire a sharp image allowing at the same time enough light to impinge on the sensor. The quality of the acquired images can be improved by attempting to achieve the highest depth of field (DOF) possible by reducing the lens aperture diameter and the focal length or increasing the stand-off distance. Adjusting the above parameters to achieve a higher frame rate and image quality reduces the number of photons that impinge on the sensors leading to the necessity to provide a high intensity illumination. To guarantee correct imaging of the target it is necessary to use a uniform light source set-up in a position that avoids shadows on the specimen. During the development of the methodology it was observed that the best solution was to use cold light sources. These sources of illumination avoid heating of the specimen by thermal radiation and the image distortion caused by waves of hot air crossing the measurement field due to conduction.

### 2.3 High speed tensile loading

The high speed tests are performed using an Instron VHS 1000, servo-hydraulic tensile test machine. The Instron VHS is a high speed servo-hydraulic test machine able to develop actuator speeds from quasi-static up to 20 m/s. The machine works by accumulating oil at a pressure of 280 bar in a pressure tank regulated by a proportional valve. This valve is controlled by a system that releases energy to move the actuator at the required testing speed. The actuator is capable of developing a force of 80 kN. To obtain a velocity of 20 m/s, an actuator acceleration travel of 150 mm is required. The load is recorded with a piezoelectric Kistler load cell that relies on a resonant load measuring system, which, as described by Wang et al. [8], might cause load cell ringing. During the actuator acceleration phase the specimen must not be clamped or loaded, but, when the desired testing speed is achieved the specimen must be instantly loaded, to do so the slack adaptor system shown in Figure 1 was developed. The specimen is clamped, using a jaw system, to a rod fitted inside a cylinder connected to the tensile test machine actuator (Figure 1a). When the actuator moves the cylinder is driven with

it but freely moves around the rod (Figure 1b). When the cylinder reaches the end of the rod a lock system engages the two elements, which now are both driven by the machine actuator, and the specimen is loaded (Figure 2c).

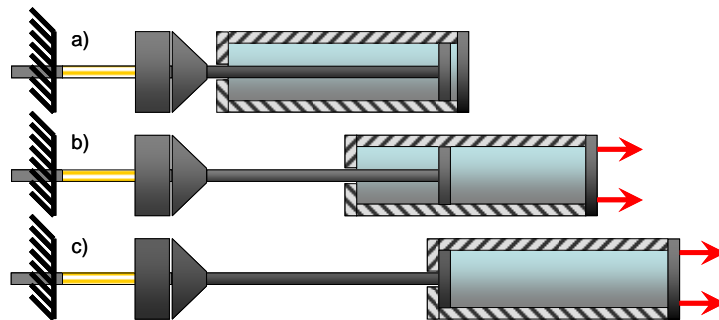


**Figure 1.** Slack Adaptor System:

- a) The actuator is in the uppermost position, the specimen is not loaded.
- b) The actuator accelerates; the cylinder and the specimen are not engaged
- c) The actuator reaches the desired speed; the cylinder engages with the specimen that it is loaded.

#### 2.4 Specimen preparation

The specimens were manufactured from a pre-preg system composed of MTM28-1 epoxy resin reinforced with E-GLASS-200 fibre. The material, supplied by Advanced Composites Group Ltd, is laminated with a unidirectional lay up, with a thickness of six plies. The pre-preg was cured at a constant pressure of 5 bar and two temperature steps of 1 hour at 90 and 120°C. A schematic of the specimens is shown in Figure 2.

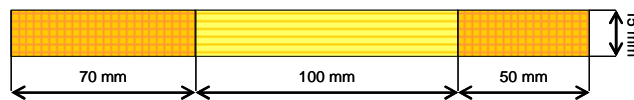


**Figure 2.** Schematic of the specimen

The size of the end-tabs was chosen to guarantee the maximum gripping surface and to localise the gauge length in an area accessible by the camera field of view when the specimen is placed in the Instron VHS. The end-tabs are integrated with the specimen during the curing by adding plies in the stacking sequence at the two extremities of the specimen. To be able to cure a laminate with a variable thickness also the vacuum bag lay-up was modified adding extra tool to maintain an adequate curing pressure over the whole laminate surface to avoid bending of the material during the cure, as shown in Figure 3.

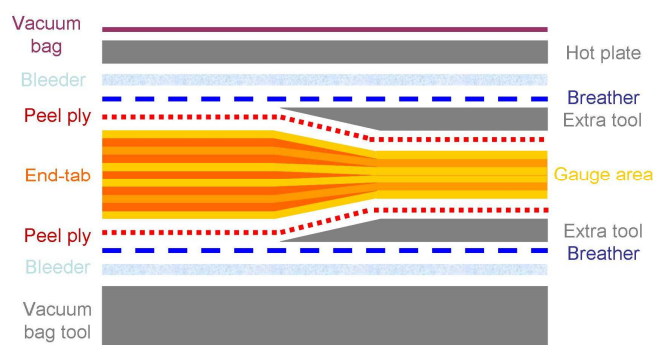


**Figure 3.** Schematic of the vacuum bag lay-up to produce co-cured end-tab specimens.

All the specimens were equipped with CEA-06-240UZ-120 Vishay strain gauges. For the DIC, spray paint from RS Components was used to create a white background and black speckles, as shown in Figure 4a. For GM, the grid, with a pitch of 0.256 mm, was transferred on the specimens using E504 epoxy adhesive by Epotecny, as shown in Figure 4b.

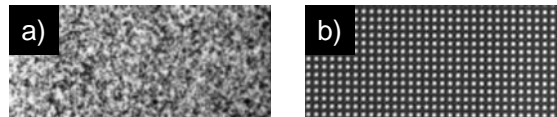


**Figure 4.** Surface preparation for full-field optical techniques:  
 a) Digital Image Correlation (DIC)  
 b) Grid Method (GM)

### 2.5 Experiment set-up

The lay out of the experimental set-up is presented in Figure 5. The Instron VHS is controlled by a computer that has a 4 channel data recording system. This system is used to record the load and the actuator displacement data directly from the machine. At the same time the system is used to record the strain gauge signal from a Vishay 2300 conditioning signal amplifier. The camera captures a pre-selected number of frames after receiving the triggering signal. As the test machine data recording and the image acquisition systems cannot be directly connected, a system to synchronise the images with the corresponding loads was developed. A pulse generator simultaneously triggers the VHS data acquisition system and the high speed camera. The triggering threshold is set by the actuator displacement signal: when the specimen is close to being loaded the triggering signal is sent. In this way, knowing the sampling rate of the data acquisition system and of the camera, it is possible to synchronise the frame with the corresponding load.

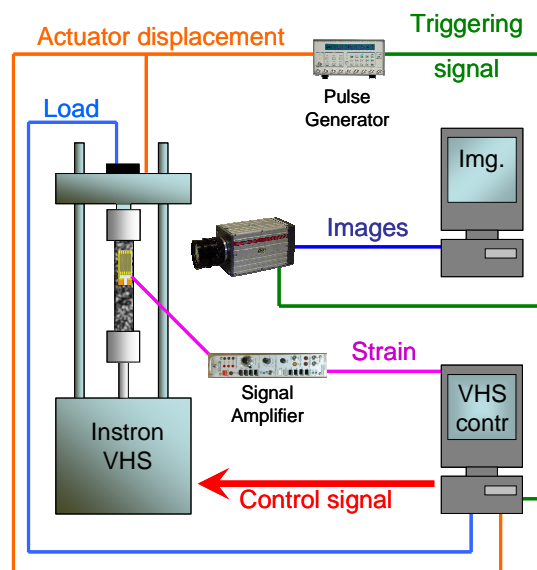


**Figure 5.** Experimental set-up

## 3 Experimental work

To prove the validity of the experimental methodology described above, a characterisation campaign was run on unidirectional GFRP specimens. These experiments also allowed a comparison of the DIC and the GM to be made. The tests were carried out on two sets of 14 specimens, one for the DIC and one for the GM. Groups of 4 specimens were tested at actuator speeds of 8 mm/s, 2 and 8 m/s; that correspond to nominal strain rates of 0.08, 20 and 80 s<sup>-1</sup>, beside this two specimens for each set were tested at a quasi-static strain rate. The images were captured using a Photron SA1 high speed camera operated at a sampling rate of 20 kHz. The data acquisition system of the Instron VHS has a sampling rate of 200 kHz. The main characteristics of the optical strain measurement techniques are summarised in Tables 1 and 2.

|                            |                             |
|----------------------------|-----------------------------|
| Technique                  | Digital Image Correlation   |
| Interrogation cell size    | 16 x 16 pixel               |
| Interrogation cell overlap | 0 %                         |
| Number of passes           | 3                           |
| Camera                     | Photron SA1, 8-bit          |
| Lens                       | Nikkor 28-105 mm f/3.5-4.5D |
| Sensor size                | 1280 x 192 pixel            |
| Field of view              | 115 x 17 mm                 |
| Frame rate                 | 20 kHz                      |
| Strain                     |                             |
| Measurement points         | 71 x 12                     |
| Spatial resolution         | 1.41 mm                     |
| Strain resolution          | 10.6 $\mu$ s                |

**Table 1.** DIC characteristics.

|                    |                             |
|--------------------|-----------------------------|
| Used Technique     | Grid Method                 |
| Grid Pitch         | 0.254 mm                    |
| Grid sampling      | 5 pixel per period          |
| Camera             | Photron SA1, 8-bit          |
| Lens               | Nikkor 28-105 mm f/3.5-4.5D |
| Sensor size        | 1280 x 192 pixel            |
| Field of view      | 115 x 17 mm                 |
| Frame rate         | 20 kHz                      |
| Strain             |                             |
| Measurement points | 256 x 38                    |
| Spatial resolution | 0.39 mm                     |
| Strain resolution  | 10.4 $\mu$ s                |

**Table 2.** GM characteristics.

### 3.1 Experimental results

As the strain field is uniform over the specimen surface (Figure 6), the stress-strain curves are constructed using the mean strain. The Young's Moduli are calculated using a linear regression of the stress-strain curves and are provided in Table 3. This set of experiments demonstrated the effectiveness of the experimental methodology, in the experimental set-up and in the specimen design. It is possible to construct the stress-strain curves for the various actuator speeds and identify the strain-rate dependent Young's modulus. Furthermore the values calculated with the two different optical techniques, DIC and GM, are in good agreement between each other and with the "control results" given by the strain gauge (SG). It is possible to observe a trend in the Young's modulus value with the increase of actuator speed and therefore of the strain rate. The value constantly increases with the increment of the strain rate, a consistent change in its value is evident between the 8 mm/s and the 2 m/s, and is attributable to a change in the deformation mechanism activated by the different speed of deformation.

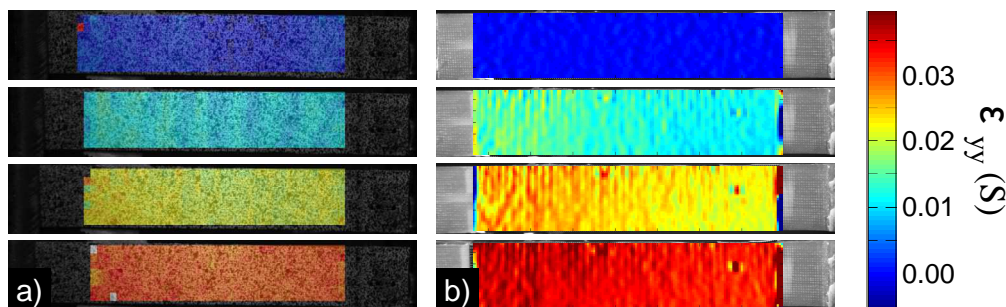


**Figure 6.** Strain maps evolution from DIC (a) and GM (b)

| Spc   | Quasi Static |       |       | 8 mm/sec |       |       | 2 m/s |       |       | 8 m/s |       |       |
|-------|--------------|-------|-------|----------|-------|-------|-------|-------|-------|-------|-------|-------|
|       | DIC          | GM    | SG    | DIC      | GM    | SG    | DIC   | GM    | SG    | DIC   | GM    | SG    |
| 1     | 38.4         |       | 38.1  | 38.7     |       | 40.6  | 43.3  |       | 42.8  | 43.4  |       | 43.1  |
| 2     | 38.7         |       | 38.0  | 39.0     |       | 39.4  | 43.4  |       | 43.0  | 42.7  |       | 42.9  |
| 3     |              |       |       | 39.6     |       | 40.6  | 41.7  |       | 42.1  | 42.9  |       | 42.7  |
| 4     |              |       |       | 38.8     |       | 39.3  | 42.0  |       | 41.6  | 42.9  |       | 43.2  |
| 5     |              | 36.5  | 38.4  |          | 39.4  | 39.6  |       | 42.6  | 42.8  |       | 42.9  | 42.7  |
| 6     |              | 36.2  | 38.5  |          | 39.1  | 39.4  |       | 43.6  | 43.2  |       | 43.1  | 43.4  |
| 7     |              |       |       |          | 39.7  | 38.8  |       | 41.7  | 41.3  |       | 42.8  | 43.4  |
| 8     |              |       |       |          | 40.4  | 40.0  |       | 42.1  | 42.7  |       | 43.3  | 43.1  |
| Avr.  | 38.55        | 36.35 | 38.25 | 39.03    | 39.65 | 39.71 | 42.60 | 42.50 | 42.56 | 42.98 | 43.03 | 43.06 |
| S. D. | 0.21         | 0.21  | 0.24  | 0.40     | 0.56  | 0.64  | 0.86  | 0.82  | 0.53  | 0.30  | 0.22  | 0.28  |

**Table 3.** Young's modulus in [GPa] summary

Comparing the characteristics of the two full-field strain measurement techniques, Table 1 and 2, it appears evident that the resolution, i.e. the capability to discern the noise from the real strain, of the two methods is comparable. The GM, however, offer a greater number of data points and has a better spatial resolution. From a practical point of view the GM requires a higher attention when setting up the experiments to correctly capture the grid and get useful images for the strain evaluation. It is in the interest of the experimenter to choose the best technique considering on one hand the longer preparation time required by the GM and on the other the higher numbers of recorded data points that this methodology allows.

#### 4 Conclusions

During the development of the experimental methodology the following observations were made:

- The co-cured end-tabs are an ideal solution for manufacturing specimens suitable for high speed tensile testing;
- The Slack Adaptor System ensures a correct loading of the specimen and reduces the out of plane movement of the specimen;
- Cold light sources reduce any alteration of the material behaviour caused by the measurement process;
- It is recommended to maximise the sampling frequency of the data acquisition system and the camera frame rate;
- It is necessary to reach the right compromise between the spatial and the temporal resolution of the camera.

Furthermore the effectiveness of the experimental methodology is proved by the good agreement of the Young's Moduli evaluated using the different optical strain measurement techniques and the strain gauges. It was observed that the two techniques offer the same strain resolution but the GM is able to provide a higher spatial resolution and therefore of data points. The experimental results show that the methodology has the potential to be a valuable tool to characterise and model the strain rate dependent behaviour of composite materials. After defining the methodology an extensive experimental characterisation campaign has been undertaken to fully exploit the strain rates achievable with the Instron VHS and collect data for input into a GFRP materials constitutive model.

## Acknowledgements

This project is funded by EPSRC, Engineering and Physical Sciences Resource Council, and DSTL, Defence Science & Technology Laboratory. The author wishes to thank the EPSRC Engineering Instrument Pool, that provided part of the imaging equipment.

## References

- [1] Okoli I. The effects of strain rate and failure modes on the failure energy of fibre reinforced composites. *Compos Struct*, **54**, pp. 299–303 (2001).
- [2] Hsiao H.M., Daniel I.M. Strain rate behaviour of composite materials. *Composites Part B*, **29B**, pp.521–33 (1998).
- [3] Cantwell W.J., Morton J. The impact resistance of composite materials: a review. *Composites*, **22**, pp. 347–62 (1991).
- [4] Sierakowsky R.L., Strain rate effects in composites. *Appl Mech Rev*, **50(11)**, pp. 741–61 (1997).
- [5] Hamouda A.M.S., Hashmi M.S.J. Testing of composite materials at high rates of strain: advances and challenges. *Journal of Materials Processing Technology*, **77(1-3)**, pp. 327-336 (1998).
- [6] Sierakowski R.L., Strain rate effects in composites. ASME, (1997).
- [7] Bardenheider R., Rogers G. Dynamic Impact Testing. Instron, (2003).
- [8] Wang W., Makarov G., and Sheno R.A. An analytical model for assessing strain rate sensitivity of unidirectional composite laminates. *Composite Structures*, **69(1)**, pp. 45-54, (2005).
- [9] Fitoussi J., Meraghni F., Jendli Z., Hug G., and Baptiste D. Experimental methodology for high strain-rates tensile behaviour analysis of polymer matrix composites. *Composites Science and Technology*, **65(14)**, pp. 2174-88 (2005).
- [10] Shokrieh M.M., Omid M.J. Tension behaviour of unidirectional glass/epoxy composites under different strain rates. *Composite Structures*, **88(4)**, pp. 595-601 (2009).
- [11] Grediac M. The use of full-field measurement methods in composite material characterization: interest and limitations. *Composites Part A: Applied Science and Manufacturing*, **35(7-8)**, pp. 751-761 (2004).
- [12] Grediac M. Importance of full-field measurement techniques for better models in solid mechanics. *Experimental Analysis of Nano and Engineering Materials and Structures*, pp. 13-14 (2007).
- [13] Pan, B., Qian, K., Xie H., Asundi A. Two-dimensional digital image correlation for in-plane displacement and strain measurement: a review. *Measurement Science and Technology*, **20(6)**, pp. 1-17 (2009).
- [14] Badulescu C., Grediac M., Mathias J.D., Roux D. A Procedure for Accurate One-Dimensional Strain Measurement Using the Grid Method. *Experimental Mechanics*, **49(6)**, pp. 841-854, (2009).
- [15] Badulescu C., Grediac M., Mathias J.D. Investigation of the grid method for accurate in-plane strain measurement. *Measurement Science and Technology*, **9**, pp. 1-17, (2009).
- [16] Pannier Y., Avril S., Rotinat R., Pierron F. Identification of Elasto-Plastic Constitutive Parameters from Statically Undetermined Tests Using the Virtual Fields Method. *Experimental Mechanics*, **46(6)**, pp. 735-755 (2006).